

# PROCEEDINGS OF SPIE

[SPIDigitalLibrary.org/conference-proceedings-of-spie](https://spiedigitallibrary.org/conference-proceedings-of-spie)

## Design status of ASPIICS, an externally occulted coronagraph for PROBA-3

Renotte, Etienne, Alia, Andres, Bemporad, Alessandro, Bernier, Joseph, Bramanti, Cristina, et al.

Etienne Renotte, Andres Alia, Alessandro Bemporad, Joseph Bernier, Cristina Bramanti, Steve Buckley, Gerardo Capobianco, Ileana Cernica, Vladimir Dániel, Radoslav Darakchiev, Marcin Darmetko, Arnaud Debaize, François Denis, Richard Desselle, Lieve de Vos, Adrian Dinescu, Silvano Fineschi, Karl Fleury-Frenette, Mauro Focardi, Aurélie Fumel, Damien Galano, Camille Galy, Jean-Marie Gillis, Tomasz Górski, Estelle Graas, Rafał Graczyk, Konrad Grochowski, Jean-Philippe A. Halain, Aline Hermans, Russ Howard, Carl Jackson, Emmanuel Janssen, Hubert Kasprzyk, Jacek Kosiec, Serge Koutchmy, Jana Kovačičinová, Nektarios Kranitis, Michał Kurowski, Michał Ładno, Philippe Lamy, Federico Landini, Radek Lapáček, Vít Lédl, Sylvie Liebecq, Davide Loreggia, Brian McGarvey, Giuseppe Massone, Radek Melich, Agnes Mestreau-Garreau, Dominique Mollet, Łukasz Mosdorf, Michał Mosdorf, Mateusz Mroczkowski, Raluca Muller, Gianalfredo Nicolini, Bogdan Nicula, Kevin O'Neill, Piotr Orleański, Marie-Catherine Palau, Maurizio Pancrazzi, Antonios Paschalis, Karel Patočka, Radek Peresty, Irina Popescu, Pavel Psota, Mirosław Rataj, Jan Rautakoski, Marco Romoli, Roman Rybecký, Lucas Salvador, Jean-Sébastien Servaye, Cornel Solomon, Yvan Stockman, Arkadiusz Swat, Cédric Thizy, Michel Thomé, Kanaris Tsinganos, Jim Van der Meulen, Nico Van Vooren, Tomáš Vit, Tomasz Walczak, Alicja Zarzycka, Joe Zender, Andrei Zhukov, "Design status of ASPIICS, an externally occulted coronagraph for PROBA-3," Proc. SPIE 9604, Solar Physics and Space Weather Instrumentation VI, 96040A (28 September 2015); doi: 10.1117/12.2186962

**SPIE.**

Event: SPIE Optical Engineering + Applications, 2015, San Diego, California, United States

# Design status of ASPIICS, an externally occulted coronagraph for PROBA-3.

Etienne Renotte<sup>a</sup>, Andres Alia<sup>a</sup>, Alessandro Bemporad<sup>h</sup>, Joseph Bernier<sup>a</sup>, Cristina Bramanti<sup>l</sup>, Steve Buckley<sup>g</sup>, Gerardo Capobianco<sup>h</sup>, Ileana Cernica<sup>q</sup>, Vladimir Dániel<sup>d</sup>, Radoslav Darakchiev<sup>j</sup>, Marcin Darmetko<sup>i</sup>, Arnaud Debaize<sup>a</sup>, François Denis<sup>a</sup>, Richard Desselle<sup>a</sup>, Lieve de Vos<sup>c</sup>, Adrian Dinescu<sup>q</sup>, Silvano Fineschi<sup>h</sup>, Karl Fleury-Frenette<sup>a</sup>, Mauro Focardi<sup>s</sup>, Aurélie Fumel<sup>a</sup>, Damien Galano<sup>t</sup>, Camille Galy<sup>a</sup>, Jean-Marie Gillis<sup>a</sup>, Tomasz Górski<sup>k</sup>, Estelle Graas<sup>a</sup>, Rafał Graczyk<sup>i</sup>, Konrad Grochowski<sup>l</sup>, Jean-Philippe Halain<sup>a</sup>, Aline Hermans<sup>a</sup>, Russ Howard<sup>v</sup>, Carl Jackson<sup>g</sup>, Emmanuel Janssen<sup>a</sup>, Hubert Kasprzyk<sup>j</sup>, Jacek Kosiec<sup>k</sup>, Serge Koutchmy<sup>w</sup>, Jana Kovačičinová<sup>e</sup>, Nektarios Kranitis<sup>f</sup>, Michał Kurowski<sup>l</sup>, Michał Ładno<sup>i</sup>, Philippe Lamy<sup>u</sup>, Federico Landini<sup>s</sup>, Radek Lapáček<sup>d</sup>, Vít Lédle<sup>e</sup>, Sylvie Liebecq<sup>a</sup>, Davide Loreggia<sup>h</sup>, Brian McGarvey<sup>g</sup>, Giuseppe Massone<sup>h</sup>, Radek Melich<sup>e</sup>, Agnes Mestreau-Garreau<sup>t</sup>, Dominique Mollet<sup>c</sup>, Łukasz Mosdorf<sup>l</sup>, Michał Mosdorf<sup>l</sup>, Mateusz Mroczkowski<sup>j</sup>, Raluca Muller<sup>q</sup>, Gianalfredo Nicolini<sup>h</sup>, Bogdan Nicula<sup>b</sup>, Kevin O'Neill<sup>g</sup>, Piotr Orleński<sup>l</sup>, Marie-Catherine Palau<sup>l</sup>, Maurizio Pancrazzi<sup>s</sup>, Antonis Paschalis<sup>f</sup>, Karel Patočka<sup>d</sup>, Radek Peresty<sup>d</sup>, Irina Popescu<sup>q</sup>, Pavel Psota<sup>c</sup>, Mirosław Rataj<sup>i</sup>, Jan Rautakoski<sup>t</sup>, Marco Romoli<sup>f</sup>, Roman Rybecký<sup>d</sup>, Lucas Salvador<sup>a</sup>, Jean-Sébastien Servaye<sup>a</sup>, Cornel Solomon<sup>p</sup>, Yvan Stockman<sup>a</sup>, Arkadiusz Swat<sup>n</sup>, Cédric Thizy<sup>a</sup>, Michel Thomé<sup>a</sup>, Kanaris Tsinganos<sup>f</sup>, Jim Van der Meulen<sup>c</sup>, Nico Van Vooren<sup>c</sup>, Tomáš Vit<sup>e</sup>, Tomasz Walczak<sup>m</sup>, Alicja Zarzycka<sup>m</sup>, Joe Zender<sup>t</sup>, Andrei Zhukov<sup>b</sup>.

a) Centre Spatial de Liège (CSL), University of Liege, Liege, Belgium; b) Solar-Terrestrial Center of Excellence (SIDC), Royal Observatory of Belgium, Brussels, Belgium; c) OIP Sensor Systems n.v., Oudenaarde, Belgium; d) Serenum a.s., Praha, Czech Republic; e) Institute of Plasma Physics ASCR v.v. i. (TOPTEC), Turnov, Czech Republic; f) National and Kapodistrian University of Athens, Athens, Greece; g) SensL Technologies Ltd., Cork, Ireland; h) INAF – Astrophysical Observatory of Torino, Italy; i) Centrum Badań Kosmicznych Polskiej Akademii Nauk, Warsaw, Poland; j) Astri Polska Sp.z.o.o., Warsaw, Poland; k) Creotech Instruments S.A., Piaseczno, Poland; l) N7 Mobile sp. z o.o., Warsaw, Poland; m) PCO S.A., Warsaw, Poland; n) Solaris Optics S.A., Jozefow, Poland; p) AE Electronics S.A., Bacau, Romania; q) National Institute for Research & Development in Microtechnologies (IMT), Bucharest, Romania; r) University of Florence, Florence, Italy; s) INAF – Astrophysical Observatory of Arcetri, Florence, Italy; t) European Space Research and Technology Centre, Noordwijk, The Netherlands; u) Laboratoire d'Astrophysique de Marseille, Marseille, France; v) Naval Research Laboratory, Washington, USA; w) Institut d'Astrophysique de Paris, Paris, France

## ABSTRACT

The “sonic region” of the Sun corona remains extremely difficult to observe with spatial resolution and sensitivity sufficient to understand the fine scale phenomena that govern the quiescent solar corona, as well as phenomena that lead to coronal mass ejections (CMEs), which influence space weather. Improvement on this front requires eclipse-like conditions over long observation times. The space-borne coronagraphs flown so far provided a continuous coverage of the external parts of the corona but their over-occluding system did not permit to analyse the part of the white-light corona where the main coronal mass is concentrated. The proposed PROBA-3 Coronagraph System, also known as ASPIICS (Association of Spacecraft for Polarimetric and Imaging Investigation of the Corona of the Sun), with its novel design, will be the first space coronagraph to cover the range of radial distances between  $\sim 1.08$  and 3 solar radii where the magnetic field plays a crucial role in the coronal dynamics, thus providing continuous observational conditions very close to those during a total solar eclipse.

PROBA-3 is first a mission devoted to the in-orbit demonstration of precise formation flying techniques and technologies for future European missions, which will fly ASPIICS as primary payload. The instrument is distributed over two satellites flying in formation (approx. 150m apart) to form a giant coronagraph capable of producing a nearly perfect eclipse allowing observing the sun corona closer to the rim than ever before.

The coronagraph instrument is developed by a large European consortium including about 20 partners from 7 countries under the auspices of the European Space Agency. This paper is reviewing the recent improvements and design updates of the ASPIICS instrument as it is stepping into the detailed design phase.

**Keywords:** PROBA-3, ASPIICS, solar physics, coronagraph, formation flying, in-orbit demonstration.

# 1. INTRODUCTION

## 1.1 Mission objectives

PROBA-3 is a mission devoted to the in-orbit demonstration (IOD) of precise formation flying ( $F^2$ ) techniques and technologies for future ESA missions. It is part of the overall ESA IOD strategy and it is implemented by the Directorate of Technical and Quality management (D/TEC) under a dedicated element of the General Support Technology Programme (GSTP). In order to complete the end-to-end validation of the  $F^2$  technologies and following the practice of previous Proba missions, PROBA-3 includes a primary payload that exploits the features of the demonstration. In this case it is a giant 150 m sun coronagraph capable of producing a nearly perfect eclipse allowing observing the sun corona closer to the rim than ever before. The coronagraph is distributed over two satellites flying in formation. The so called coronagraph satellite (CSC) carries the “detector” and the so called occulter satellite (OSC) carries the Sun occulter disc. A secondary payload will be embarked on the occulter satellite: the DARA solar radiometer.

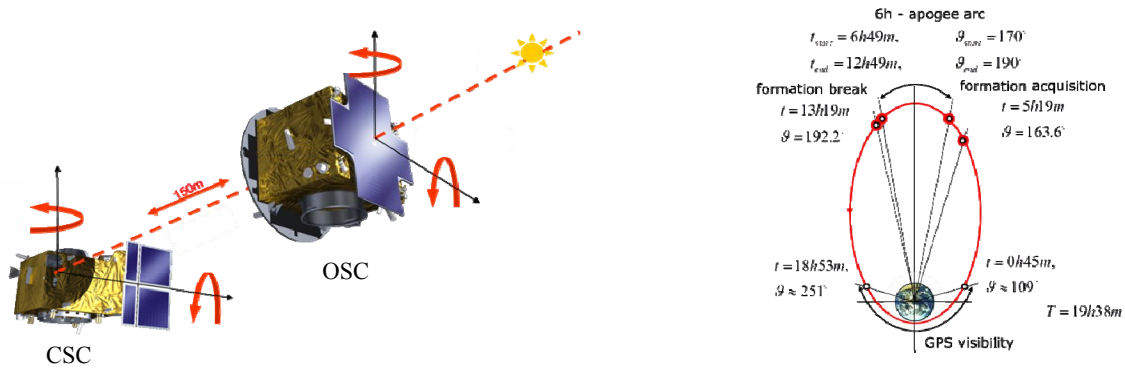


Figure 1: PROBA-3 formation flying overview and orbit.

## 1.2 ASPIICS Coronagraph

The region within the sonic point (around 2 – 3 solar radii from the solar centre), where the solar wind is accelerated and coronal mass ejections (CMEs) are initiated, remains extremely difficult to observe with spatial resolution and sensitivity sufficient to understand these phenomena. This requires eclipse-like conditions for long periods of time. However natural eclipses do not allow studying the coronal dynamics and eruptive phenomena during a sufficient amount of time to analyse its magnetic structure and the ubiquitous processes of dissipation of the free magnetic energy. Space-borne coronagraphs were designed and flown to provide a continuous coverage of the external parts of the corona but their over-occluding system did not permit to analyse the part of the white-light corona where the main coronal mass is concentrated.

The proposed PROBA-3 Coronagraph, also known as ASPIICS (Association of Spacecraft for Polarimetric and Imaging Investigation of the Corona of the Sun), will be the first space coronagraph to cover the range of radial distances between ~1.08 and 3 solar radii ( $R_{Sun}$ ), thus providing continuous observational conditions very close to those during a total solar eclipse, but without the effects of the Earth’s atmosphere. The ASPIICS unprecedented field of view makes it uniquely suited for studies of the solar corona, as it will fill the crucial observational gap between the fields of view of low-corona EUV imagers and conventional space coronagraphs. ASPIICS will combine observations of the corona in both natural and polarized white light [540nm – 570nm] with images of prominences in the He I line (587.6nm) and Fe XIV line (530.3nm).

ASPIICS will provide novel solar observations to achieve two major solar physics science objectives: 1°) to understand physical processes that govern the quiescent solar corona and 2°) to understand physical processes that lead to coronal mass ejections (CMEs) and determine space weather.

## 2. INSTRUMENT DESIGN

### 2.1 Overview

ASPIICS optical design follows the general principles of a classical externally occulted Lyot coronagraph. The external occulter (EO), hosted by the Occulter Spacecraft (OSC), blocks the light from the solar disc while the coronal light passes through the circular entrance aperture of the Coronagraph Optical Box (COB), accommodated on the Coronagraph Spacecraft (CSC). A general sketch of the Coronagraph System is shown in Figure 2.

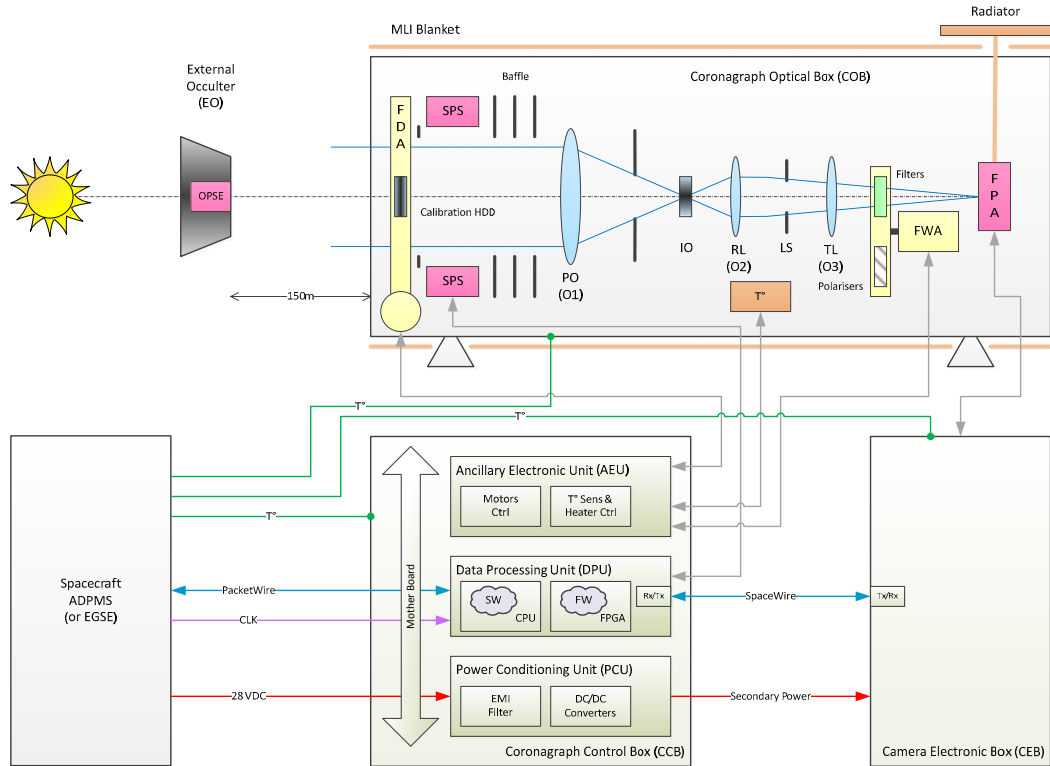


Figure 2. Coronagraph system functional block diagram.

The Coronagraph instrument is made of four units:

- The Coronagraph Optical Box (COB),
- The Coronagraph Control Box (CCB),
- The Camera Electronic Box (CEB), and
- The Occulter Position Sensor Emitters (OPSE), located on the OSC.

The science objectives have driven the following key design requirements for the coronagraph:

- To perform white-light coronal observations within a useful field of view from 1.08 to 3 solar radii  $R_{\text{sun}}$  with a minimum spatial resolution of 5.6 arcsec (plate scale  $\leq 2.8$  arcsec/pixel).
- To perform coronal polarimetric imaging in the [540 – 570nm] band, by measuring the linear polarisation state along at least three different directions of polarization: 0, +60, -60 degrees.
- To perform narrow-band imaging of prominences and the surrounding coronal material in the He I D3 emission line at 587.6 nm ( $\Delta\lambda = 2.0$  nm)
- To perform narrow-band imaging of the corona in the Fe XIV emission line at 530.3 nm ( $\Delta\lambda = 2.0$  nm).

## 2.2 Optics

The Coronagraph optical system consists in a Primary Objective (PO) that forms an image of the external occulter (EO) onto the internal occulter (IO). The IO is slightly oversized to block the diffraction from the EO and to take into account the possible co-alignment error between the two spacecraft's. The field lens O2 makes a real conjugate image of the entrance pupil on the Lyot stop, in order to block the diffraction coming from the pupil's edges. The imaging lenses (O3 + Tele lens) make an image of the solar corona on the detector.

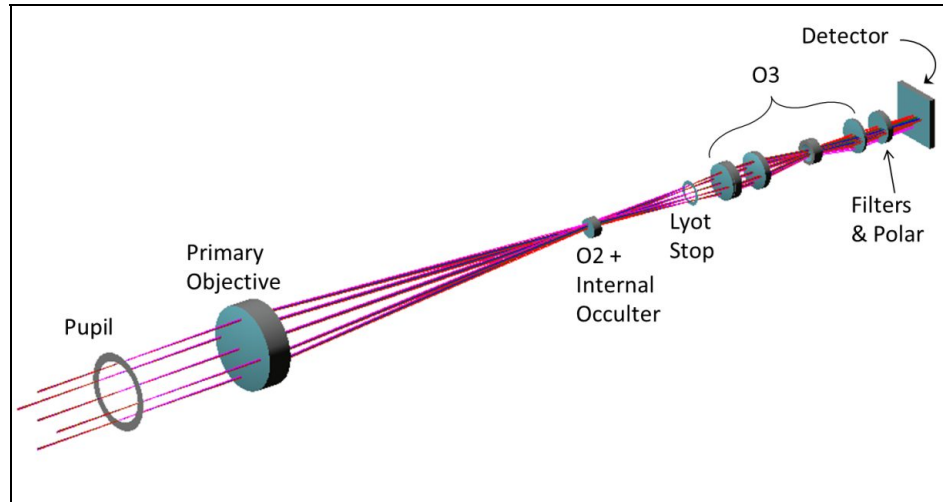


Figure 3. Coronagraph System Lens Objectives.

The PO is a doublet composed of a BK7G18 lens in optical contact with a N-SF8 lens. The molecular bonding of the two lenses limits the creation of ghosts. The front lens is made of radiation hard glass to avoid any darkening effects. The primary objective has been optimized for a finite object distance (EO at 144.348 m) and for a field angle corresponding to the edge of the EO ( $1.02 R_{\text{Sun}}$ ). The field lens O2 is a SF6 plano-convex lens. The lenses group O3 is composed of four individual lenses. It creates an image of the sun corona and reduces the divergence of the beam when crossing the filters and polarizers to avoid chromatic issues.

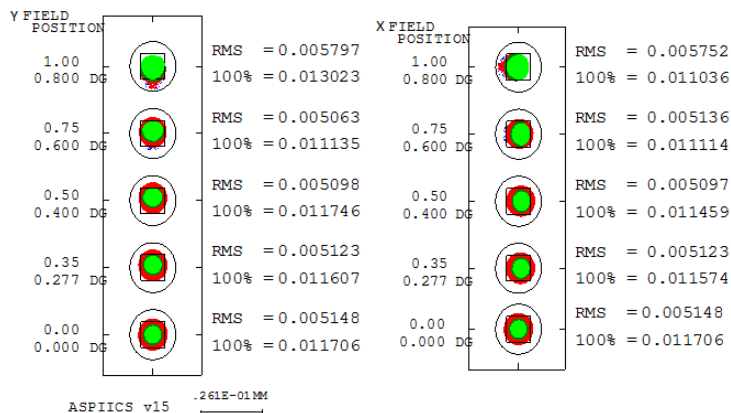


Figure 4. Image spot diagrams at focal plane.

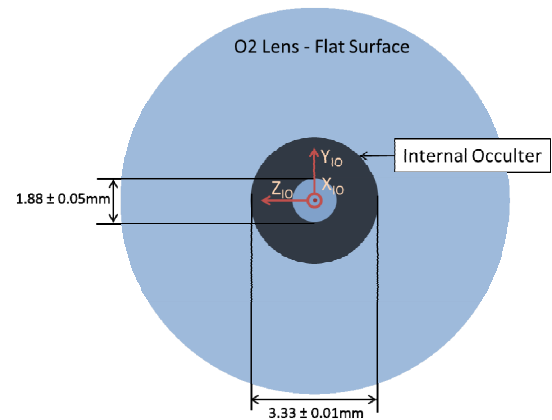


Figure 5. IO design (typical dimensions).

The IO is designed to block the diffraction produced by the edge of the EO. It consists of a coating deposited on the O2 Lens, with a central hole so that the instrument can acquire images of the OPSE lights (see below). The minimum dimension of the IO is when its size is directly the size of the conjugate image of the EO ( $\approx 1.02 R_{\text{Sun}} = 0.272^\circ$ ). In this configuration, the IO radius shall be  $R_{\text{io}} = 1.631\text{mm}$ , corresponding to an angular dimension of 1014.6 arcsec (equivalent to  $1.057 R_{\text{Sun}}$  but this is given for information only since it has no real meaning, the IO being not conjugated with the Sun). During sensitivity analysis, several over-occultation scenarios have been considered, to take into account different tolerances (EO misalignment, stray-light, etc.) yielding to an actual IO size between 1.798mm and 1.874mm in

radius. Finally, the Lyot stop is designed to block the diffracted light produced by the pupil edges. It is mounted on the relay lens O<sub>3</sub> barrel. The Lyot Stop aperture is 11.4mm in diameter.

In terms of image quality, the optical tolerance analysis demonstrated RMS spots  $\leq 5.8 \mu\text{m}$  at the border of the field of view (diffraction limit:  $19.36 \mu\text{m}$  at 540nm). The overall calculated transmission of the instrument is  $> 70\%$  in the useful wavelength range. Additional details on the ASPIICS optical design, modelling and performance can be found the companion paper [10].

The principal source of stray light is the Sun light diffracted by the EO edge. Subsequently, the main contributors to the straylight are the ghosts from reflections between the optics and the scattering by the optics. The straylight induced by the scattering on the mechanical parts is several orders of magnitude lower than the two previous contributors.

### Filters & polarisers

A filter wheel mechanism (see below) allows placing the following filters and polarisers in front of the detector:

- Broad-band filter 540-570 nm,
- 3 Polarizing Broad-band filter 540-570 nm (filter combined with a linear polarizer),
- Narrow-band filter Fe XIV at 530.3 nm ( $\Delta\lambda = 2 \text{ nm FWHM}$ ),
- Narrow-band filter He I D3 at 587.6 nm ( $\Delta\lambda = 2 \text{ nm FWHM}$ ),
- 

### High density filter

A high density diffuser (HDD) composed of a ground fused silica plate is used to produce a flat field on the detector plane when lit by the Sun, with a flux compatible with the dynamics of the coronagraph. The HDD is located in the lid of the Front Door Assembly.

## 2.3 Detection chain

### Focal plane assembly

The Focal Plane Assembly (FPA) consists of a front-side illuminated CMOS Active Pixel Sensor (APS), the proximity electronics of the APS, a harness from the FPA to the Camera Electronic Box (CEB), the FPA mechanical parts, a passive radiator and its thermal strap. The selected image sensor is a CMOS APS, manufactured by CMOSIS (Belgium) that has been developed for the ISPHI instrument of Solar Orbiter. No additional qualification testing or other development aimed at improving the performance of the proposed sensor will be envisaged in the context of this mission.

Table 1. Image sensor specifications.

Array	2048 x 2048
Package	PGA
Type	Front side illuminated
Pixel size	10 $\mu\text{m}$ x 10 $\mu\text{m}$
Spectral range	400 nm to 800 nm
QE	$> 50\%$
Operational temperature	$< -40^\circ\text{C}$
Read-out noise	60 e-
Dark current	$< 20\text{e-}/\text{px}/\text{s}$
Fixed pattern noise	$< 20\text{e-}$
Full well	114 ke-
Dynamic range	66 dB
Frame rate	10FPS
Pixel output rate	64 MHz
Windowing	along 1 direction
Readout mode	Rolling shutter
TID	$> 100 \text{ krad}$
Power consumption	0.5 W

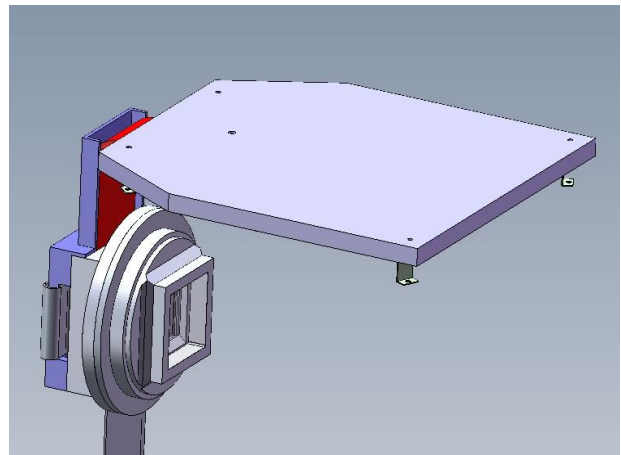


Figure 6. Coronagraph system focal plane assembly with radiator (Phase B design).

The sensor is configurable through a SPI line. The pixel array of the sensor requires to be clocked externally. The output of the sensor is analogue. The sensor is powered from the secondary voltage of the CCB. The APS proximity electronics

is a front-end printed circuit board aimed at supporting the image sensor electrically but also mechanically. It contains elements for biasing (capacitors, resistors), decoupling (capacitors), and communication to the CEB (drivers, buffers). A radiator is used to cool down passively the FPA so that the sensor can operate in a lower temperature range for noise reduction purposes. The radiator will be connected to the mechanical housing by means of a thermal strap.

### Image data handling

The high dynamic in the coronal images is managed electronically while minimizing telemetry requirements. The proposed strategy is to take several images, subdivided in blocks (also called “image tiles”), with different exposure times (typically 0.1, 1 or 10 seconds) and recombine them on the ground (Figure 7). The image tile data are transferred to the CCB “on-the-fly” as they are available so that they don’t need to be stored inside the CEB memory after formatting.

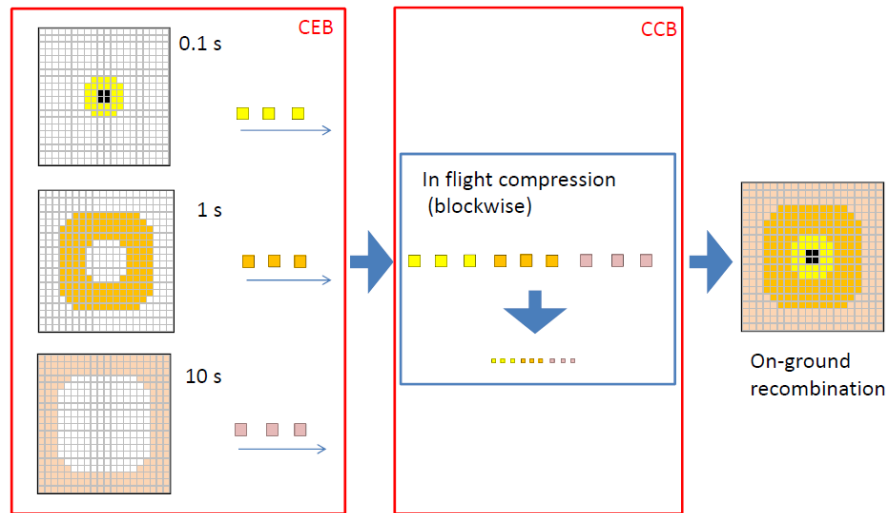


Figure 7. Image data handling principle.

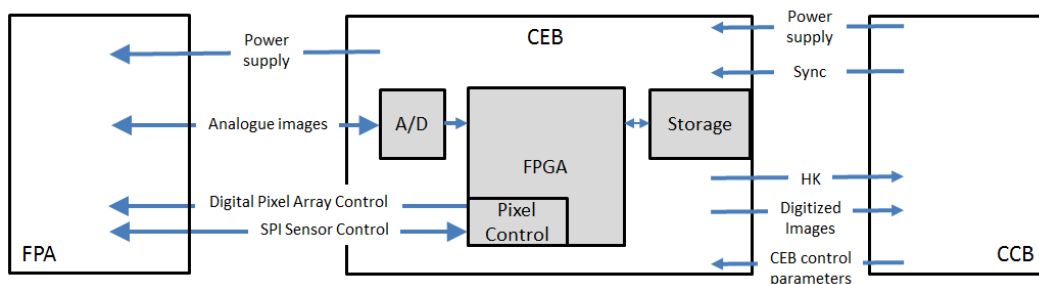


Figure 8. CEB functional diagram.

### Camera electronic box

The Camera Electronic Box (CEB) is dedicated to controlling the FPA. It interfaces with the FPA on one side, to which it sends the necessary control signals and receives in return the analogue pictures from the CMOS APS; with the CCB on the other side, from which it receives its configuration and to which it sends housekeeping and digitized pictures. Upon trigger from the CCB, the CEB starts an image acquisition and is able to acquire, handle and buffer up to three full exposures (2048×2048 pixels) with configurable exposure times. The CEB divides the full exposures acquired by the FPA into square blocks of 64×64 pixels and transfers to the CCB only those blocks defined in the current observation mask, while discarding other blocks. The CEB also performs basic image quality checks (overexposed/underexposed pixels counting and flagging).

## 2.4 Mechanical structure

The coronagraph structure is based on a tube and a box mounted on 3 feet (Figure 9). The feet are made of Titanium alloy and consist of 3 bipods (more exactly 2 bipods and 2 monopods). They ensure isostatic mounting to decouple mechanically the optical box from the spacecraft optical bench. The feet also ensure thermal insulation to limit heat load from and towards the optical bench ( $\sim 6\text{mW/K}$  per foot). The monopods are located under the tube and the bipods on the equipment box sides. The tube holds the first part of the optical elements. The entrance pupil is located at the very front of the instrument to avoid any mechanical element in front of it. In the centre of the tube, the primary objective is inserted. This objective images the Corona on an intermediate focus and the external occulter on the internal occulter. It is important to maintain the internal occulter at an accurate position to ensure that it continuously covers the external occulter image. A suitable distance is maintained between the pupil and the primary objective in order to protect the lenses from direct view of bright elements in space, to protect it from radiation and to ensure that the temperature between the objective and the internal occulter remains stable and uniform. The full tube is thermally controlled by a

heater. At the front of the tube, the Front Door Assembly is attached in order to protect the tube interior and more particularly the front lenses from contamination. In flight the door will also reduce the risk of long exposure to direct Sun (un-occulted), this can be detrimental for the detector and cause important increase of temperature. The door will also be used in flight for calibration of the optical system. In the middle of the cover lid, a diffuser will spread the light of the Sun in the entire field of view in order to distribute it uniformly on the detector. A number of vanes are inserted in the tube in order to prevent straylight from source out of the field of view to enter the optical system.

The second part of the structure is a box holding the different optical elements. The equipment box also contains the filter wheel. This wheel holds the filters and polarisers for the different observation modes. The filters in the wheel are tilted in order to ensure that no ghost is generated by the flat surfaces. The FPA is mounted on the back wall of the box. It includes the detector matrix and thermal links to the externally mounted radiator. The Equipment Box is also thermally regulated.

## 2.5 Mechanisms

### Filter Wheel Assembly

The Filter Wheel Assembly (FWA) is a 6-position mechanism designed to position the combination of filters and polarisers described above within the science beam between O3 and the FPA. A stepper motor with a 5:1 gear box rotates the wheel during position change and ensures fixation of the wheel during exposures. Sets of 4 cams are placed at the rear side of the filter wheel. They engage magneto-resistive sensors when the appropriate working filter is placed into the beam. To reduce vibration during launch and during rotation of the disc the counter bearing assembly is designed.

### Front Door Assembly

The Front Door Mechanism is designed to protect telescope optics from contamination on the ground, during launch and some flight operations and to avoid thermal loads of inner part of coronagraph. The Front Door Assembly (FDA) has two operational positions and one locked position. During launch, the Lid is locked by a wax pin-puller and protects the optics and detector from direct sun light. During the non-observation phases of Coronagraph instrument, the lid is in the

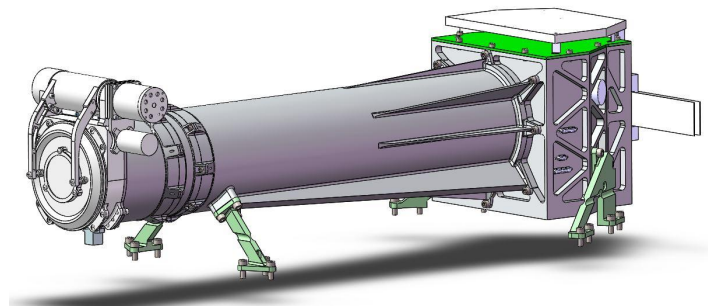


Figure 9. Coronagraph COB overview.

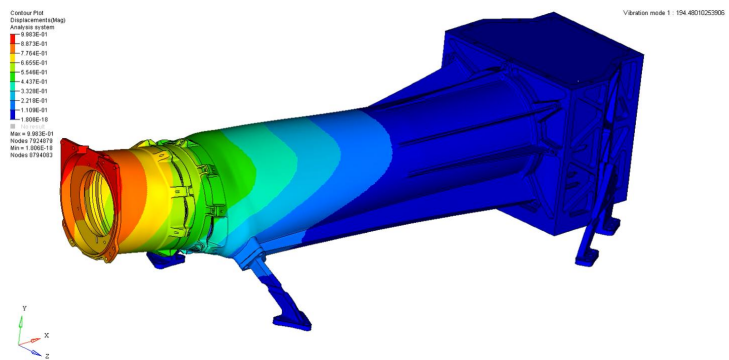


Figure 10. COB first mode (194.5Hz).

closed position. Before and after the Coronagraph observation the Lid is moved by stepper motor via gearbox to the Open position.

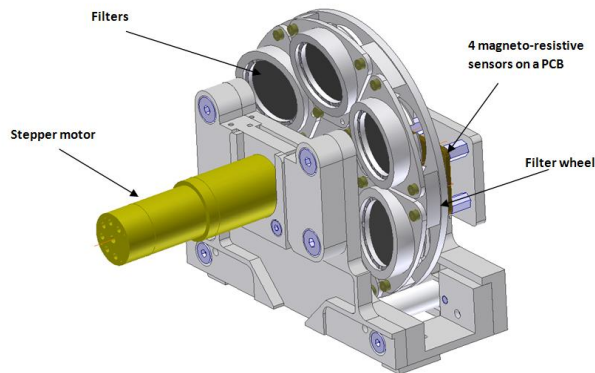


Figure 11. Filter Wheel Assembly (FWA).

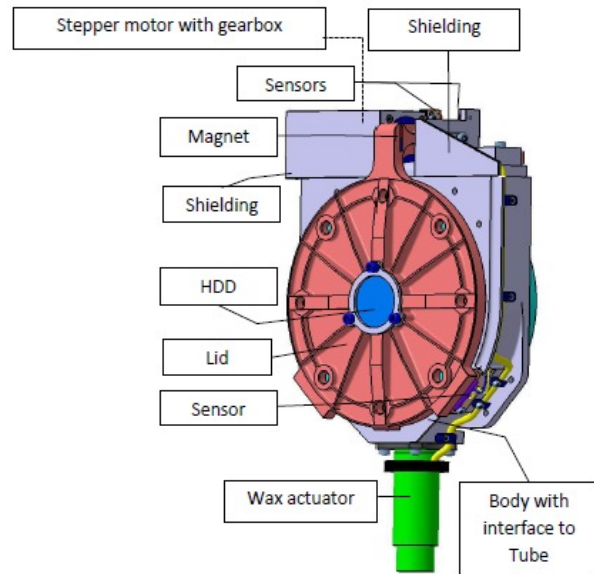


Figure 12. Front Door Assembly (FDA).

## 2.6 External occulter

The external occulter (EO) is a critical element for coronagraphs as it is the major stray light source. The external occulter shape must be optimized in order to reduce the light that is diffracted by its edge and then scattered by the telescope optics. The issue is so delicate that dedicated preliminary investigations have been performed and are described in [3], [4], [6], and [13] that we recommend to refer for more detailed information. According to the preliminary studies, the current baseline optimization is a truncated cone (see Figure 13), from 70 to 100 mm thick and with a semi-angle that has to respect the following constraints:

- the truncated cone surface must be in the shadow of the EO outer edge with respect to the solar disk light.
- The cone surface must be as close as possible (compatibly with pointing uncertainties) to the line connecting the IEO outer edge and the pupil edge.

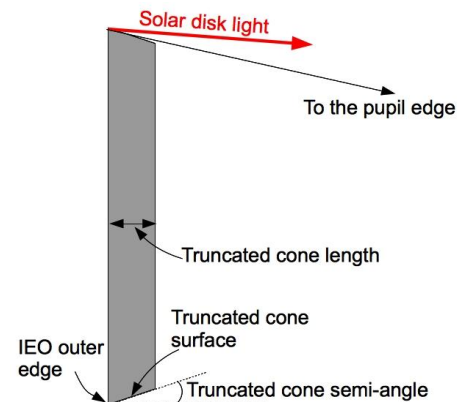


Figure 13. EO geometry.

According to investigation results, such optimizations would reduce by at least a factor two the level of diffracted light inside the entrance pupil of the coronagraph [5], [13]. The EO outer edge shall be as smooth as possible, in order to prevent solar disk light scattering from manufacturing imperfections. The EO surface must be black coated and with a Lambertian surface finishing.

## 2.7 Formation flying metrology

### Shadow position sensor

The Shadow Positioning Sensors (SPS), together with the Occulter Position Sensors Emitter (OPSE) form the ASPICS metrology units. The SPS verifies the safe centring of the entrance pupil of the coronagraph within the shadow cone formed by the occulting disc. Initially planned for a high sensitivity relative measurement of the umbra location with reference to the centre of the entrance pupil of the coronagraph instrument, it has evolved towards a sensor giving an

absolute location with a high accuracy. Another function required on the SPS is to signal to the satellite that the umbra moves away from nominal position, this is to prevent the risk of full Sun illumination inside the coronagraph instrument.

Eight light sensors are used (Figure 14). The sensors are equally distributed on a 55 mm radius circle centred on the entrance pupil. The output current response expected by the SPS is computed in the penumbra around the location of SPS on the entrance pupil plane (Figure 15). The illumination in the penumbra has been computed for three cases: by neglecting the limb darkening (solid line), by including the limb darkening (dashed line) and by adding to the limb darkening a sunspot located at the limb (dotted line).

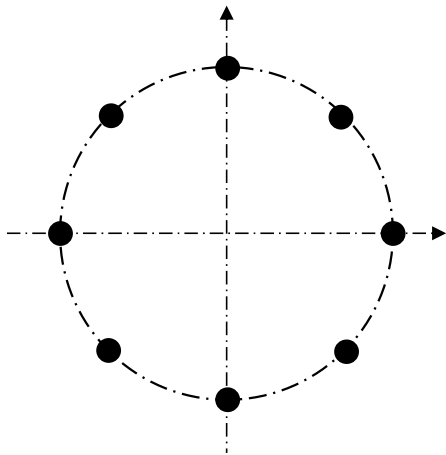


Figure 14: SPS photodiode arrangement around entrance pupil.

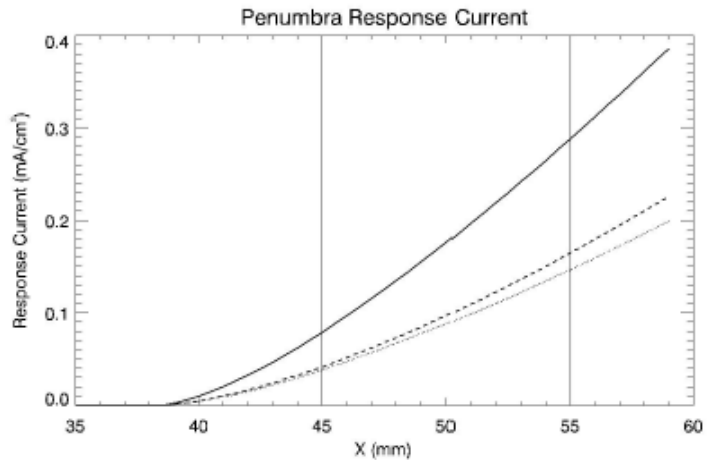


Figure 15: SPS response current in the penumbra on the entrance pupil plane as a function of the distance from the telescope optical axis.

From the 2D distribution of the SPS response currents, it is then possible to estimate the sensitivities necessary to detect the occulter displacements in agreement with performance requirements, i.e.

- for lateral displacements, a sensitivity of 0.45% with diodes at 55 mm is needed to meet the lateral measurement accuracy of 50 $\mu$ m (3- $\sigma$ ) in each axis;
- for longitudinal displacements, a sensitivity of 0.048% with diodes at 55 mm is needed to meet the longitudinal measurement accuracy of 1mm (3- $\sigma$ ).

This shows that the requirement on longitudinal displacement is more challenging (by about one order of magnitude) than the requirement on lateral displacement. The SPS is developed as a joint effort of INAF (Torino, Italy) and SensL Ltd. (Cork, Ireland). Please refer to [11] and [12] for further details on the SPS design and performance.

### Occulter position sensor emitters

The purpose of the OPSE is to verify the positioning of the occulting disc in the field-of-view of the coronagraph that is the alignment of both spacecrafts independently of the pointing to the Sun. The OPSE consists of a set of 3 light emitters mounted on the rear side of the external occulting disc. Their images produced by the coronagraph have a characteristic pattern that uniquely defines the position along the transverse axes, with respect to the instrument coordinate system. Moreover an estimate of the inter-satellite distance (ISD) and of the orientation of the external occulter is also delivered. The 3 OPSE are located close to the centre of the disk, limiting by this way the size of the central hole of the IO. The images of the OPSEs are received by the FPA and are sent to ground for analysis, like other images. (The information delivered by the OPSE is therefore not usable onboard in real time.) The use of the OPSE supposes a coronagraph fully operational, door open, with the entrance pupil in the umbra or low penumbra. Each of the three OPSE enclosures integrates two LEDs of two types, so four LEDs per enclosure. The use of two LEDs with different central wavelengths decreases the main risk of a light wavelength falling out of the spectral band of the coronagraph. Indeed, at least one of the two LEDs must emit in the band pass of the white-light filter (540-570 nm) of the coronagraph, and the major problem is that the central wavelength of a LED slightly shifts with temperature. The temperature of the rear side of the occulting disc is estimated close to -117 °C but with a large uncertainty. The LEDs selected, at the moment, are the one from Phase B: the models VS575N and VS590N from OPTRANS CORP (Japan) which emits respectively at 575 nm

and 590 nm at +25 °C. Preliminary tests have been performed at IMT-Bucharest to characterize these two LEDs (and others) with temperature: wavelength drift, output power drift and forward current-voltage drift. The drift of central wavelength of VS575N for an operating temperature close to -133 °C (140 K) leads to a working wavelength close to 559 nm which is in the wavelength band of the CI. The peak wavelength of this LED is shifted by 0.07 nm/°C to the lower wavelength when the temperature decreases. The same coefficient was found for the VS590N. (This is lower than the 0.2 nm/°C considered in Phase B and could lead to use only one LED instead of the 2 LEDs planned initially.) The OPSE image properties have been studied to verify the light distribution at the focal plane and the vignetting of the IO; the radiometric budget has also been estimated. From these studies the SNR has been evaluated for different output powers of the LEDs (from 0.15 mW to 1 mW at room temperature). By considering the VS575N LED that has an output power of ~ 0.15 mW measured by IMT, the SNR is always above 100 for the LED emission angle of ± 6°. Note that a PWM at 50% was considered in this analysis. The accuracy requirement for the measurement of the lateral and longitudinal displacement has also been retrieved. In order to reach an accuracy on the lateral displacement measurement of 300 μm (3σ) the centroiding accuracy has to be 1.3 μm (1/8 of a pixel). For the longitudinal displacement measurement of 210 mm (3σ), the centroiding accuracy has also to be 1.3 μm. Some centroiding algorithms have been studied to check the monitoring of the OPSE Point Spread Function (PSF) movements, with the expected SNR. The most common procedure, centre of gravity and the fit to analytical models are well suited to guarantee the expected performances of the OPSE system. Further details can be found in [14].

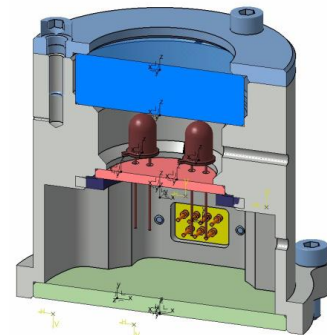


Figure 16. OPSE design, courtesy of LAM.

## 2.8 Electronics and software

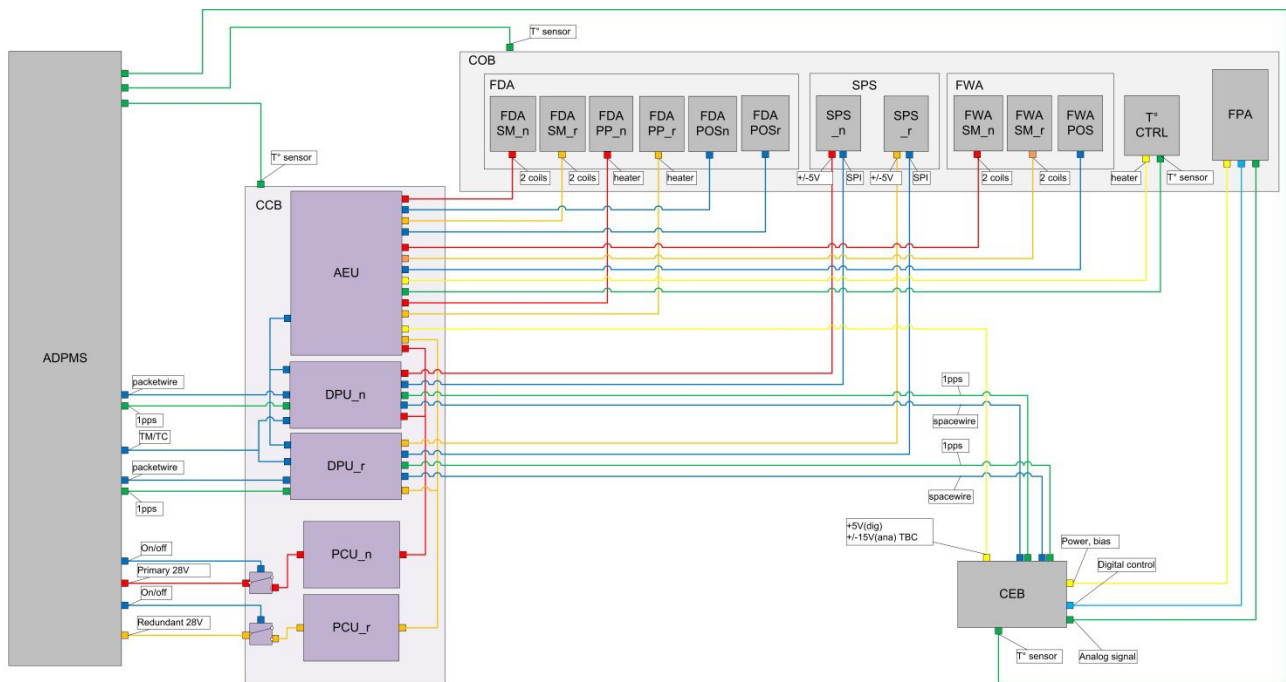


Figure 17. ASPIIC electrical architecture.

## Coronagraph control box

The Coronagraph Control Box (CCB) is the electronic controller of the coronagraph. It consists of an electronic box including:

- Power conditioning unit (PCU): a power supply module that provides all the voltages required by CI. PCU is switched on at the moment when ADPMS provides power, and supplies DPU and AEU instantaneously,
- Data processing unit (DPU): a control and data processing modules that can also store some resulting data. DPU has data / control link to ADPMS, CEB and AEU auxiliary board.
- Ancillary electronics unit (AEU): a board containing switches, turning on and off subsystems of the instrument, ADCs and stepper motor controls. AEU switches are controlled directly by DPU.

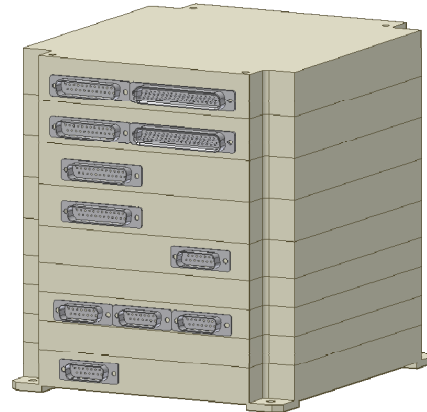


Figure 18. Coronagraph Control Box (CCB).

The DPU is responsible for Coronagraph control and management functionality. It consists of two main functional parts, a System-on-Chip microcontroller GR712RC that hosts complete 2-core LEON3 microprocessor (CPU) with peripherals and a configurable logic device (FPGA) to implement data processing functionality and processor peripherals which are missing in GR712RC. DPU has several types of memory. Its purpose is to store and execute application code and to store and process scientific data. Memories in principle are connected to microprocessor. Additionally, there is envisioned a cache memory connected to FPGA that will be used for scientific telemetry packet assembly. CPU will have SRAM or MRAM for operation system, application execution needs. Up to 1GB of SDRAM can be implemented to act as scientific mass memory (volatile) before sending the scientific data to ADPMS (through DPU FPGA). This could be a memory space where additional scientific algorithms execute, if necessary. Small, non-volatile flash memory will be used to hold boot loader and, both, basic and application software images. An RTAX 2000 FPGA contains the CCSDS compressor engine (see below), some cache buffers and Packet Wire interface and additional peripherals. In order to give CPU full control over what happens in FPGA, for communication between CPU an FPGA SpaceWire with RMAP will be used. With such solution, AMBA bus connecting all IP cores in external FPGA is “mapped” in address space of microprocessor, so there is a straightforward access to all IP cores, to configure them and program DMA transfers. Interrupts from IP cores residing in FPGA will be fed to processor via GPIOs. Data arrives in CPU via SpaceWire, and it has either to be stored in temporary memory and later fed to FPGA or, as in fact, we will have to use separate SpaceWire interfaces in microprocessor, to receive the data from CEB and to control the FPGA, a DMA mechanism is involved in data reception, so no temporary storage would be involved.

## On-board Software

CCB software is structured into two separate programs: Boot Software (BSW) and Application Software (ASW). Both programs are compiled separately and are independent meaning that only one can be executed at a time. Software is executed by CCB Data Processing Unit (DPU) based on Leon3 processor. In general BSW provides functionalities related to bootloader. Main functionalities are summarized below.

- Performing initial built-in self-test (BIST)
- Generation of boot report
- FDIR handling with dedicated Safe Mode
- Detailed self-tests of CCB modules
- ASW booting/updating
- Simplified packetization and PUS packets handling

BSW will provide possibility to boot selected ASW image from two images stored in MRAM. First image will be the default image preloaded on ground. There will be no possibility of updating this image during flight. Second image will be updatable with BSW software management functions. BSW will provide only possibility to update whole image. Main functionalities of the ASW are summarized below.

- Commanding Coronagraph modules (AEU, FDA, FWA, LCVR, PCU, COB, CEB, CCSDS-RICE)

- Instrument mode management
- Image acquisition when requested by ADPMS
- Image data handling and buffering
- Packetization and PUS handling
- Shadow Position Sensor (SPS) algorithms calculations

## 2.9 Image data compression

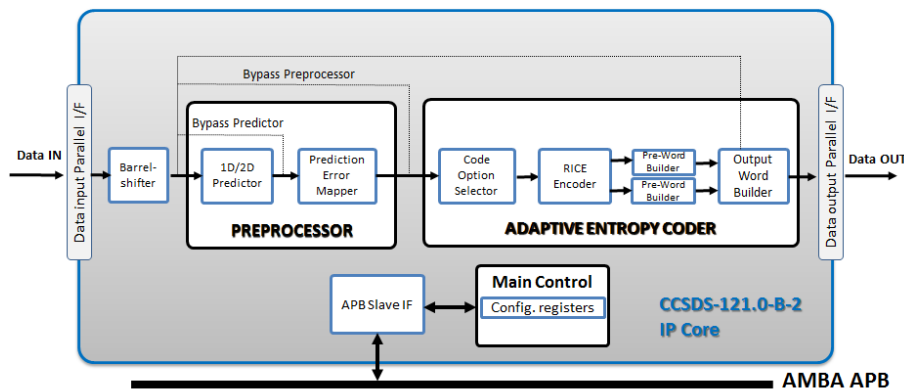


Figure 19. Image data compression IP core block diagram.

ASPIICS implements both lossless and near-lossless compression capabilities, selectable by ground command. The Image Data Compressor (IDC) is based on the CCSDS 121.0-B-2 algorithm and consists of an IP Core firmware to be implemented on the CCB RTAX 2000 FPGA. The top level architecture of the IDC IP Core consists of two major processing units (Figure 19): preprocessor and adaptive entropy coder along with a Main Control unit which hosts the configuration registers [15]. The Image Data Compressor IP Core configuration registers are memory mapped, accessible by the AMBA APB bus through a Slave APB interface and therefore they can be accessed by standard serial link interfaces like SpaceWire-RMAP or SPI. Compression ratios near 3 and up to 9 can be reached for 12 bits/pixel dynamic range with the lossless and near-lossless compression options, respectively.

## 3. INSTRUMENT PERFORMANCE

### 3.1 Field of view ( $R_{Sun}$ )

The “ $R_{Sun}$  performance” is a key requirement of the coronagraph. It is defined as the smallest field angle, expressed in solar radius, that the instrument can image. The goal is to reach a minimum FoV of  $1.08 R_{Sun}$  (50%-vignetted image) for an EO angular size of  $1.02 R_{Sun}$  and inter-satellite distance of 144.348 m. There are, however, various contributors to the  $R_{Sun}$  error. The major ones are the stray-light ( $\Delta R_{Sun} \sim 0.065 R_{Sun}$ ) and spacecraft misalignment ( $\Delta R_{Sun} \sim 0.047 R_{Sun}$ ). The combination of all error sources imposes oversizing the IO and leads to a current estimate of the  $R_{Sun}$  performance ( $3\sigma$ ) of  $1.22 R_{Sun}$  (50%-vignetted image) and  $1.16 R_{Sun}$  if systematic errors can be corrected for. This performance will be investigated further in order to keep the inner edge of the field of view as close to the solar surface as possible.

### 3.2 Optical performance

Table 2. Instrument optical characteristics and performance.

Entrance pupil diameter:	$\varnothing 50$ mm
Instrument focal length:	734.687 mm
Geometrical field of view (with vignetting):	$1.043 - 3 R_{Sun}$ (EO = $1.02 R_{Sun}$ )
Geometrical field of view (w/o vignetting):	$1.117 - 3 R_{Sun}$ (EO = $1.02 R_{Sun}$ )
Useful wavelength range:	540, 555, 570, 590 nm
Diffraction limit @ 540 nm:	$\varnothing 19.36 \mu\text{m}$
Maximum distortion:	-0.19%
Geometrical image quality at Focal Plane:	RMS Spot < $5.8 \mu\text{m}$ @ 540 nm
Sensitivity (tolerance analysis):	RMS Spot < $6.4 \mu\text{m}$ @ 540 nm, @ $3R_{Sun}$

### 3.3 Engineering budgets

Table 3. Instrument engineering budgets.

CSC Mass (COB + CEB + CCB + Harnesses):	24.1 kg (incl. contingency)
OSC Mass (3 OPSEs):	0.7 kg (incl. contingency)
COB Dimensions (L × W × H):	882.4 mm × 339.4 mm × 232 mm (ext. envelope)
CCB Dimensions (L × W × H):	180 mm × 200 mm × 170 mm (excl. connectors)
CEB Dimensions (L × W × H):	165 mm × 95 mm × 51 mm (excl. connectors)
Power consumption (stand-by / observation / peak):	26 W / 38.6 W / 49 W
Telemetry (typical mix of observations):	~16 Gbits/week

## 4. DEVELOPMENT PLAN

### 4.1 Programmatics

A previous study (Phase B), led by *Laboratoire d'Astrophysique de Marseille (LAM)*, was completed in spring 2013 and the project has been restarted in July 2014 on the basis of a new industrial structure reflecting the redistribution of resources allocated to this programme. This paper is presented after a nearly one year design consolidation phase whilst the ASPIICS project is transiting into Phase C/D/E1. ASPIICS is built by a European consortium including about twenty partners from seven countries (Belgium, Poland, Romania, Italy, Ireland, Greece, and The Czech Republic) under the auspices of the European Space Agency's General Support Technology Programme (GSTP) and the Czech Prodex Programme. The planned Phase C/D duration is 2½ years with an expected launch date in late 2018.

### 4.2 Model philosophy

The model philosophy that we will apply to support the development of our instrument is summarised in Table 4. It serves both our internal needs for validating critical technologies and the needs expressed at Mission level to populate the spacecraft models. The principal “de-risking model” is the DM that will consist of a complete functional prototype of the telescope.

Table 4. Instrument model philosophy summary.

Model	Representativeness	Consortium Use	Customer Use
Development Model (DM)	Partially representative, depending on the technology to be validated	For validation of sub-unit key technologies For developing and end-to-end breadboard of the COB for F <sup>2</sup> metrology ancillary units validation	To support the Mission formation flying metrology needs
Structural-Thermal Model (STM)	Thermo-mechanical representative (mounting interface, mass properties, structural properties, thermal properties, envelope and shape, subsystems structural & thermal dummies, harness)	For math models correlation, to populate upper-level STM and support system level tests	To support the Mission STM programme
Engineering (Qualification) Model (EQM)	Flight representative (full flight design & flight standard with respect to electrical, optical, and mechanical parameters) NOTE: EM/EQM shall be composed at least of EQM for the Coronagraph Optical Box (COB) elements and Focal Plane Assembly (FPA), whereas electronics could be proposed at EM or EQM level depending the criticality of the qualification of the units	For qualification, to verify performances, functional interfaces and operational procedures, to validate functional interfaces at instrument level, and to populate and support system-level qualification	To support the Mission EM/EQM programme
Proto Flight Model (PFM)	Full flight design & flight standard	For acceptance testing, and to populate instrument FM	The flight hardware & software
Flight Spare (FS)	A sensible kit of spare components/sub-assemblies (flight standard)	For quick replacement of failed/damaged flight hardware	For quick replacement of failed/damaged flight hardware

### 4.3 Verification plan

The qualification test baseline is derived from ECSS-E-ST-10-03C (protoflight test baseline), which is tailored according to the equipment category and to the specific programme's needs. The proposed test matrix is presented in Table 5.

Table 5. Instrument test matrix.

Test Category	Test Content	STM	EM	EQM	PFM	Notes
General	Functional, performance	-	T	T	T	
	Life	-	-	T	-	
Physical	Mass	T	-	T	T	
	Dimensions	T	-	T	T	
	COG	A	-	A	A	By analysis only
	MOI	A	-	A	A	By analysis only
Mechanical	Random vibration	T	-	T <sub>QQ</sub>	T <sub>AA</sub> /T <sub>QA</sub>	T <sub>QA</sub> for E-Boxes
	Sine vibration	T	-	T	T	
	Shock	-	-	T	- / tbc	To be confirmed for E-Boxes
Thermal	Thermal vacuum	-	-	T <sub>QQ</sub>	T <sub>AA</sub> /T <sub>QA</sub>	T <sub>QA</sub> for E-Boxes
	Thermal Balance	T	-	T	- / T	
Electrical	EMC	-	tbc	-	T	To be confirmed for EM E-Boxes
	Magnetic	-	tbc	-	- / tbc	On EM or PFM E-Boxes (TBC)
	ESD	-	tbc	-	- / tbc	On EM or PFM E-Boxes (TBC)

QQ = Qualification level and Qualification duration/cycles ; QA = Qualification level and Acceptance duration/cycles ;  
AA = Acceptance level and Acceptance duration/cycles

## 5. SUMMARY

This paper presents the current status of ASPIICS, a solar coronagraph that is the primary payload of ESA's formation flying in-orbit demonstration mission PROBA-3. This instrument is designed as a classical externally occulted Lyot coronagraph but takes advantage of the opportunity to place the external occulter on a companion spacecraft, about 150m apart, to perform high resolution imaging of the inner corona of the Sun as close as ~1.1 solar radii. The images will be tiled and compressed on board in a one-time programmable (OTP) space qualified antifuse FPGA before being down-linked to ground for scientific analyses. ASPIICS is built by a European consortium including about twenty partners from seven countries (Belgium, Poland, Romania, Italy, Ireland, Greece, and the Czech Republic).

## 6. ACKNOWLEDGEMENTS

The ASPIICS project will be developed under the auspices of the ESA's General Support Technology Programme (GSTP) and the ESA's Prodex Programme thanks to the sponsorships of seven member states: Belgium, Poland, Romania, Italy, Ireland, Greece, and the Czech Republic.

## REFERENCES

- [1] Lamy, P., Vives, S., Damé, L., Koutchmy, S., "New perspectives in solar coronagraphy offered by formation flying: from PROBA-3 to Cosmic Vision", *Proc. SPIE 7010* (2008).
- [2] Lamy P.; Damé L.; Vives S.; Zhukov A., "ASPIICS: a giant coronagraph for the ESA/PROBA-3 Formation Flying Mission", *Proc. SPIE 7731* (2010).
- [3] Landini F.; Mazzoli A.; Venet M.; Vives S.; Romoli M.; Lamy P.; Rossi G., "Measurements and optimization of the occulting disk for the ASPIICS/PROBA-3 formation flying solar coronagraph", *Proc. SPIE 7735* (2010).
- [4] Landini F., Vives S., Venet M., Romoli M., Fineschi S., "External occulter laboratory demonstrator for the forthcoming formation flying coronagraphs", *Applied Optics*, Vol. 50, No. 36 (2011).
- [5] Vives S., et al., "Optical performances of the PROBA-3/ASPIICS solar coronagraph", *SFFMT 2013 Proc.*
- [6] Landini F. et al., "Improved stray light suppression performance for the solar orbiter/METIS inverted external occulter", *Proc. SPIE 8862* (2013).

- [7] Paschalis A., et al., "ASPIICS CCB: The functional Control Electronics of an Externally Occulted Solar Coronagraph Instrument for the ESA PROBA-3 Mission", *SFFMT 2013 Proc.*
- [8] Plesseria, J.Y. et al. "Design and development of ASPIICS, an externally occulted solar coronagraph for PROBA-3 mission." *SFFMT 2013 Proc.*
- [9] Renotte, E. et al. "ASPIICS: an externally occulted coronagraph for PROBA-3. Design evolution.", *Proc. SPIE 9143* (2014).
- [10] Galy, C. et al. "Design and Modelisation of ASPIICS Optics." *SPIE Paper Nr 9604-7* (2015).
- [11] Bemporad, A. et al. "The shadow positioning sensors (SPS) for formation flying metrology on-board the ESA-PROBA3 mission." *SPIE Paper Nr 9604-9* (2015).
- [12] Focardi, M. et al. "Formation flying metrology for the ESA-PROBA3 Mission: the shadow positioning sensors (SPS) silicon photomultipliers (SiPMs) readout electronics." *SPIE Paper Nr 9604-10* (2015).
- [13] Landini, F. et al. "Significance of the occulter diffraction for the PROBA3/ASPIICS formation flight metrology." *SPIE Paper Nr 9604-11* (2015).
- [14] Loreggia D. et al. "OPSE metrology system onboard of the PROBA3 mission of ESA". *SPIE Paper Nr 9604-12* (2015).
- [15] N. Kranitis, I. Sideris, A. Tsigkanos, G. Theodorou, A. Paschalis, R. Vitulli, "Efficient field-programmable gate array implementation of CCSDS 121.0-b-2 lossless data compression algorithm for image compression", *Journal of Applied Remote Sensing*, 9(1), 097499, May 2015, doi:10.1117/1.JRS.9.097499.